ATLAS NOTE

ATLAS-PHYS-PUB-2013-011

September 30, 2013

Prospects for benchmark Supersymmetry searches at the high luminosity LHC with the ATLAS Detector

The ATLAS Collaboration

Abstract

Supersymmetry is one of the best motivated and well-studied extensions of the Standard Model. The current searches at the LHC have yielded sensitivity to TeV scale gluinos and 1st and 2nd generation squarks, as well as to 3rd generation squarks and electro-weakinos in the hundreds of GeV mass range. The high-luminosity phase of the LHC will extend sensitivity well beyond the current limits. This document presents some example benchmark studies with a parameterised simulation of the ATLAS detector at a centre-of-mass energy of 14 TeV. In addition projections of results from 8 TeV based searches are discussed. Results are shown for integrated luminosities of 300 and 3000 fb^{-1}.

ATL-PHYS-PUB-2013-011
30 September 2013

1 Introduction

The Standard Model (SM) of particles and fields describes experimental data over a large energy range and many of its predictions have been succesfully tested at the per mille level. The SM is however considered as a low energy effective theory as the scalar sector is unstable under radiative corrections and new phenomena are expected at the TeV scale.

Supersymmetry (SUSY) [1] is a hypothetical new symmetry of Nature which relates fermions and bosons. It requires that for every boson (fermion) of the SM there exists a yet unseen fermionic (bosonic) partner. SUSY particles with masses at the electroweak scale represent the new degrees of freedom that cancel the quadratic divergences of the SM. SUSY also accommodates the unification of the gauge interactions, a radiative breaking of the electroweak symmetry, and represents an essential ingredient of superstring theories. Under the conservation of R-parity SUSY predicts the existence of a candidate for the dark matter in the Universe. Furthermore, the minimal supersymmetric model (MSSM) requires a Higgs boson with mass below ~135 GeV which could be consistent with the recently observed Higgs-like resonance [2, 3]. The discovery (or exclusion) of weak-scale SUSY is one of the highest physics priorities for the current and future LHC, including its high luminosity upgrade (HL–LHC ($\sqrt{s}$ =14 TeV; 3000 fb^{-1}). The multi-TeV energy range probed with the LHC and the HL-LHC will not be accessible at any other current or next generation facility.

This note shows comparisons of the discovery and exclusion reach of a ~300 fb^{-1} LHC and a ~3000 fb^{-1} HL-LHC for a few benchmark SUSY analyses. Although R-parity violating scenarios would also profit from the HL-LHC, this note concentrates on a few illustrative R-parity conserving scenarios.

1.1 The LHC and HL–LHC

In 2012, the LHC delivered 22.8 fb^{-1} of proton-proton collisions at a centre-of-mass-energy of 8 TeV. During the shutdown following the end of data-taking (LS1) the machine will be consolidated to be able to operate at a centre-of-mass-energy close to the design value of 14 TeV. In the following data taking period, lasting until the end of 2017, the LHC will collect ~100 fb^{-1}. A second long shutdown (LS2) will take place starting in 2018 during which the injection chain will be modified to allow for instantaneous luminosities up to ~2×10^{34} cm^{-2}s^{-1} with a 25 ns bunch spacing. The maximum average number of pile up events per bunch crossing is expected to be $\langle\mu\rangle \sim 60$. The data collected from 2020 until 2022 will amount to ~300 fb^{-1}. Around 2022, the accelerator will be upgraded to the HL-LHC which will be able to achieve luminosities of ~5×10^{34} cm^{-2}s^{-1} (LS3). The machine is expected to deliver ~3000 fb^{-1} by about 2030. The average number of pile up events per bunch crossing for the HL–LHC will be $\langle\mu\rangle \sim 140$.

1.2 The ATLAS experiment

ATLAS [4] is a multipurpose particle physics apparatus with a forward-backward symmetric cylindrical geometry and nearly 4π coverage in solid angle.[1] The layout of the detector is dominated by four superconducting magnet systems, which comprise a thin solenoid surrounding inner tracking detectors (ID) and three large toroids supporting a large muon tracker (MS). In the pseudorapidity region $|\eta| < 3.2$, high-granularity liquid-argon (LAr) electromagnetic (EM) sampling calorimeters surround the solenoid magnet. An iron-scintillator tile calorimeter provides hadronic coverage over $|\eta| < 1.7$. The end-cap and forward regions, spanning $1.5 < |\eta| < 4.9$, are instrumented with LAr calorimetry for both EM and hadronic measurements.

[1] ATLAS uses a right-handed coordinate system with its origin at the nominal interaction point in the centre of the detector and the z-axis along the beam pipe. Cylindrical coordinates (r, ϕ) are used in the transverse plane, ϕ being the azimuthal angle around the beam pipe. The pseudorapidity η is defined in terms of the polar angle θ by $\eta = -\ln\tan(\theta/2)$.

1.3 Selected results from searches for *R*-parity conserving SUSY at the LHC

In the framework of generic *R*-parity conserving supersymmetric extensions of the SM, SUSY particles are produced in pairs and the lightest supersymmetric particle (LSP) is stable. In a large fraction of the parameter space the LSP is the lightest neutralino, where neutralinos ($\tilde{\chi}_j^0$, $j = 1, 2, 3, 4$) and charginos ($\tilde{\chi}_i^{\pm}$, $i = 1, 2$) are the mass eigenstates originating from the superposition of the SUSY partners of Higgs and electroweak gauge bosons (higgsinos and gauginos). The scalar partners of right-handed and left-handed fermions can mix to form two mass eigenstates, nearly degenerate in the case of first and second generation squarks and sleptons ($\tilde{q}$ and $\tilde{l}$), whilst possibly split in the case of bottom and top squarks (sbottom, $\tilde{b}$ and stop, $\tilde{t}$) and tau sleptons (stau, $\tilde{\tau}$). The lighter stop mass eigenstate can be significantly lighter than the other squarks and the gluinos ($\tilde{g}$, supersymmetric partners of the gluons).

The searches in the initial phases of the LHC (in particular those corresponding to the 35 pb^{-1} and the 1 fb^{-1} datasets) targeted processes with large expected cross-section, such as production of gluinos and 1^{st}, 2^{nd} generation squarks (Fig. 1). As the integrated luminosity increased, the search strategy was

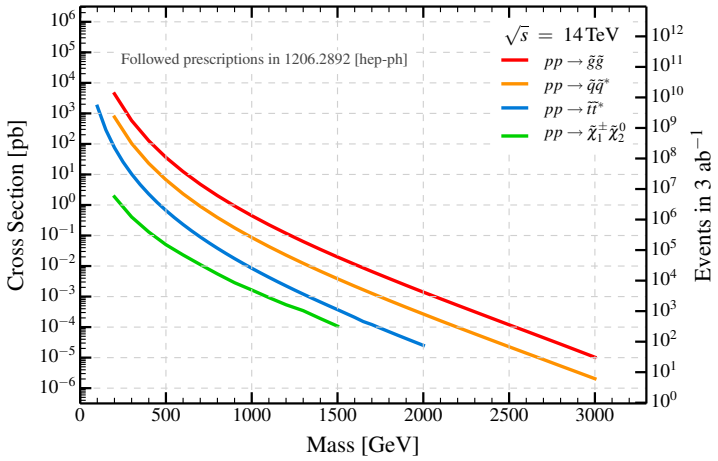

Figure 1: Next-to-leading order cross-sections for the production of supersymmetric particles at the LHC as a function of the average mass of the pair-produced supersymmetric particles. The $\tilde{\chi}_1^{\pm}$ and $\tilde{\chi}_2^0$ are assumed to be wino-like.

refined to access processes with either smaller cross-section or a-priori lower sensitivity. The ATLAS Collaboration is currently carrying out a broad programme of searches [5] including searches for light-flavour squarks and gluinos, weakly produced sparticles, and third generation squarks.

Results from the searches mentioned above have excluded 1^{st} and 2^{nd} generation squark and gluino masses below about 0.7 TeV and 1.3 TeV, respectively, under the assumption of a very light LSP [6]. Less stringent limits are placed on third generation squarks [7], weak gauginos [8] and sleptons [9]. The mass constraints strongly depend on the assumed SUSY mass spectrum.

1.4 Searches for *R*-parity conserving SUSY at the HL–LHC

If a signal of new physics is found at the LHC, the HL-LHC will be essential to determine the properties of the underlying physics and a large programme of measurements would be undertaken. This note focuses on the discovery and exclusion reach of the LHC and HL-LHC for a few illustrative examples. Further scenarios will be studied in upcoming notes.

Previous studies of the discovery and exclusion reach of the HL-LHC have been carried out for squark and gluino production, for the production of stops and for the production of charginos and neu-

tralinos [10]. A simplified model with first and second generation squarks, gluinos and low mass neutralinos was investigated. An increase of integrated luminosity from 300 to 3000 fb^{-1} allows to extend both the exclusion and discovery reach of squarks and gluinos by about 400 GeV reaching a mass of up to 3000 GeV for exclusion.

This note updates the searches for stop pair production and searches for charginos and neutralinos with improved parameterizations of the ATLAS detector, re-optimized selections and an improved estimation of all the relevant background processes. The following analyses are developed for this note:

- search for the direct production of top squarks,
- search for the direct production of a neutralino and a chargino with the decay to gauge bosons,

under the assumptions of:

- 300 fb^{-1} at $\sqrt{s}$= 14 TeV and $\langle\mu\rangle \sim 60$ (LHC)
- 3000 fb^{-1} at $\sqrt{s}$= 14 TeV and $\langle\mu\rangle \sim 140$ (HL–LHC).

For these analyses Monte Carlo generator level information is used for both the background and the signal processes. The detector response is a parameterisation based on existing data samples and full high pile-up Monte Carlo simulations of the upgraded detector, as described in Ref. [11]. The parameterizations describe the resolution and the reconstruction efficiencies of electrons, muons, tau-leptons, photons, jets, b-jets and missing transverse momentum. The parameterised response functions account for the effect of the number of multiple interactions per bunch crossing ranging between 60 and 140 with 25ns bunch spacing. The effect of the trigger is not taken into account in these analyses, but planned upgrades to the detector are expected to allow lepton and missing energy triggers that would have high efficiency for the studied scenarios with respect to the analysis selections.

In addition to the analyses using this parameterised detector response of 14 TeV Monte Carlo, projections based on current 8 TeV analyses are also considered. The background and SUSY signal expectated yields in signal regions at 8 TeV are reweighted as a function of the parton densities to 14 TeV. The expected reach is calculated for 300 and 3000 fb^{-1} at 14 TeV. Section 4 presents the projected discovery and exclusion reach for the pair production of bottom squarks and of charginos.

1.5 Monte Carlo samples

Several Monte Carlo (MC) generators are used to model the dominant SM processes and new physics signals relevant for the analyses. `SHERPA` [12] is used to simulate the top pair, diboson $WZ^{(*)}$, $W^{(*)}$+jets, and $Z^{(*)}$+jets processes. Additional dedicated `ALPGEN` [13] samples are used for the $W^{(*)}$+jets, and $Z^{(*)}$+jets processes in the search for chargino and neutralino associated production. The generator `MadGraph` [14] is used for the production of $t\bar{t}V$ ($V = W, Z$) events and the production of WWW, ZZZ and ZWW events (collectively referred to as 'triboson' or VVV in this note). The expected diboson yields are normalised to the `SHERPA` predictions. The top-quark pair-production contribution is normalised to approximate next-to-next-to-leading-order calculations (NNLO) [15]. The NNLO `FEWZ` [16, 17] cross-sections are used for normalisation of the inclusive W+light-flavour jets and Z+light-flavour jets. The expected triboson and ttV yields are normalized to NLO. The `CTEQ6L1` [18] parton distribution functions (PDFs) are used with `MadGraph` and the `CT10` [19] PDFs with `MC@NLO` and `SHERPA`.

The signal MC samples are produced with `HERWIG++` [20]. The yields are normalized to the NLO cross-section calculated with `PROSPINO`[21] in the case of electro-weakino production. They are normalized to NLO+NLL accuracy [22] for stop and sbottom production. The most relevant MC samples have equivalent luminosity (at 14 TeV) of at least 1000 fb^{-1}.

1.6 Expected sensitivity

For the analyses discussed in this document, limits are set using a significance-like variable, referred to as Z_n [23], which takes into account the systematic uncertainties on the background. The value of Z_n is required to be larger than 5 for discovery and larger than 1.64 for 95% CL exclusion [2].

The most important sources of experimental systematic uncertainties are due to the energy resolution and scale uncertainty of jets, leptons and $E_{\mathrm{T}}^{\mathrm{miss}}$; b-tagging efficiency; pile-up; and the trigger efficiency. For the dedicated studies at 14 TeV a coarse systematic uncertaintiy of 30% on the estimated sum of all backgrounds is assumed, which is consistent with the uncertainties found in published searches. The projection studies assume conservatively that the uncertainties determined for the 8 TeV analysis hold for the HL-LHC. Theoretical uncertainties on the SUSY yields due to the choice of renormalization and factorization scales and PDF are not considered in this study.

2 Search for direct production of top squarks

2.1 Physics Motivation

Naturalness arguments [24, 25] require the top squark to be light, with a mass typically below 1 TeV. At $\sqrt{s} = 14\,\mathrm{TeV}$ the direct stop pair production cross-section for 600 GeV (1 TeV) stops is 240 (10) fb. An increase in luminosity from $300\,\mathrm{fb}^{-1}$ to $3000\,\mathrm{fb}^{-1}$ increases the sensitivity to heavy stop or, if stop candidates are found, will allow to measure their properties. Stops can decay in a variety of modes which typically includes top or b quarks, W/Z or Higgs bosons, and an LSP. Pair production signatures are thus characterised by the presence of several jets, including b-jets, large missing transverse momentum and possibly leptons.

2.2 Description of the models

Among the possible scenarios, the following model is considered in this study. The pair-produced stops are assumed to decay to a top quark and the LSP ($\tilde{t} \rightarrow t + \tilde{\chi}_1^0$) with 100% branching ratio (Figure 2), requiring that $m(\tilde{t}) - m(\tilde{\chi}_1^0) > m(t)$. The final state for such a signal is characterized by a top quark pair produced in association with large missing transverse momentum from the undetected LSPs. The mixing matrices for the stop and for the neutralino LSP are chosen such that the top quark produced in the decay has a right-handed polarization in 95% of the decays. A signal grid is generated with a step size of 100 GeV both for the stop and LSP mass values.

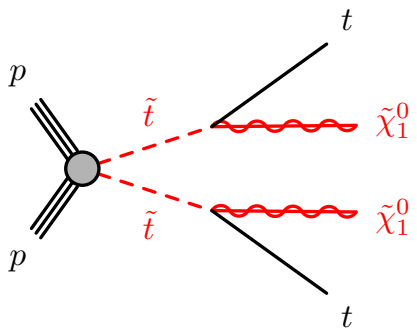

Figure 2: The Feynman diagram for the $\tilde{t} \rightarrow t + \tilde{\chi}_1^0$ simplified model studied in this note.

[2] One sided confidence interval.

2.3 Event Selection

Two studies are carried out as counting experiments targeting the $\tilde{t} \rightarrow t + \tilde{\chi}_1^0$ scenario:

- A one-lepton-based selection ($\ell \in \{e, \mu\}$) with stringent requirements on the missing transverse momentum and on the transverse mass computed from the lepton momentum and the missing transverse momentum.
- An all-hadronic selection, vetoing on the presence of leptons ($\ell \in \{e, \mu\}$), and utilizing the missing transverse momentum and the transverse mass computed from b-tagged jets and the missing transverse momentum.

The two analysis channels are mutually exclusive and the final sensitivity is based on the statistical combination of the two channels.

2.3.1 1-lepton channel optimization

The strategy follows closely the one adopted in Ref. [7]. Events are required to contain exactly one electron with $p_{\mathrm{T}} > 25$ GeV and $|\eta| < 2.5$ or exactly one muon with $p_{\mathrm{T}} > 20$ GeV and $|\eta| < 2.4$. Events containing additional electrons (muons) with $p_{\mathrm{T}} > 20(10)$ GeV and $|\eta| < 2.5(2.4)$ are rejected. Four or more jets with $p_{\mathrm{T}} > 80, 60, 40, 25$ GeV and $|\eta| < 2.5$ are required, and at least one jet has to be identified as a b-jet. The minimum azimuthal separation between either of the two highest p_{T} jets and the direction of the missing transverse momentum is required to be greater than 0.8. The hadronically decaying top quark is reconstructed by selecting the jet-jet pair with the smallest ΔR, and then adding a third jet closest in $\Delta R = \sqrt{\Delta\phi^2 + \Delta\eta^2}$ to the jet-jet pair. The three-jet mass (m_{jjj}) is required to be between 130 and 205 GeV.

Three key observables are used to define the signal regions and suppress the SM background contributions:

- the missing transverse momentum, $E_{\mathrm{T}}^{\mathrm{miss}}$;
- the transverse mass variable, $m_{\mathrm{T}} = \sqrt{2 \times p_{\mathrm{T},\ell} \times E_{\mathrm{T}}^{\mathrm{miss}} \times (1 - \cos(\Delta\phi))}$ where $\Delta\phi$ is the angular separation of the lepton and the $E_{\mathrm{T}}^{\mathrm{miss}}$.
- a variable related to the significance of the $E_{\mathrm{T}}^{\mathrm{miss}}$ measurement, defined as $E_{\mathrm{T}}^{\mathrm{miss}} / \sqrt{H_{\mathrm{T}}}$, where $H_{\mathrm{T}} = \sum_{jets=1}^{4} |\boldsymbol{p}_{\mathrm{T}}|$;

The requirements on $E_{\mathrm{T}}^{\mathrm{miss}}$, m_{T} , $E_{\mathrm{T}}^{\mathrm{miss}} / \sqrt{H_{\mathrm{T}}}$ and on the minimum p_{T} requirements for the leading 4 jets were examined across the plane of stop and LSP masses. In comparison to the requirements used in previous studies [10] looser requirements on the jet p_{T} are used while tighter requirements are placed on $E_{\mathrm{T}}^{\mathrm{miss}}$ and on m_{T} to give a better separation between signal and background, particularly for high (low) stop (LSP) mass scenarios. The $E_{\mathrm{T}}^{\mathrm{miss}}$ significance requirement is fixed to $E_{\mathrm{T}}^{\mathrm{miss}} / \sqrt{H_{\mathrm{T}}} > 15 \sqrt{\mathrm{GeV}}$, while the requirements on $E_{\mathrm{T}}^{\mathrm{miss}}$ and m_{T} are tightened as a function of stop mass. Table 1 shows the minimum requirements on $E_{\mathrm{T}}^{\mathrm{miss}}$ and m_{T} as a function of the stop mass. Numbers of events for signal and background are shown in Table 2.

Figure 3 (left) shows the $E_{\mathrm{T}}^{\mathrm{miss}}$ distribution after all other requirements have been applied, for an assumed integrated luminosity of 3000 fb^{-1}. The most important backgrounds are from dileptonic $t\bar{t}$ events where the second lepton is a hadronically-decaying τ, and from $t\bar{t}$+V (where $V = W, Z$). The $t\bar{t}$+V background is dominated by $t\bar{t}$+Z events. Background from W+jets processes is also significant.

	300 fb^{-1}		3000 fb^{-1}	
m_{stop} (GeV)	E_T^{miss} (GeV)	m_T (GeV)	E_T^{miss} (GeV)	m_T (GeV)
500	350	250	400	250
600	400	300	450	300
700	500	350	500	350
800	550	350	550	350
900	600	400	600	400
1000	650	500	700	500
1100	700	500	750	550
1200	750	500	800	550
1300	750	500	800	550
1400	750	500	800	550
1500	750	500	800	550

Table 1: Minimum requirements on E_T^{miss} and m_T for the stop search in the 1-lepton channel as a function of the stop mass, for integrated luminosities of 300 fb^{-1}and 3000 fb^{-1}.

	(800,100)	(1100,100)
$t\bar{t}$	257±25	6.6±3.8
$t\bar{t}$+W	15±2	0.9±0.5
$t\bar{t}$+Z	71±7	8.5±2.3
W+jets	41±11	5.4±3.8
Total bkg	385±28	21.4±5.9
Signal	880±18	55.7±1.5

Table 2: Numbers of events for background and two representative signal points for the 1-lepton stop analysis for an integrated luminosity of 3000 fb^{-1}. The column headings indicate the masses of the stop and of the LSP, m($\tilde{t}$,$\tilde{\chi}_1^0$), in GeV. The selection criteria are optimized to these masses. Estimates are based on MC only and uncertainties are statistical only.

2.3.2 0-lepton channel optimization

The strategy in the 0-lepton channel follows closely the one adopted in Ref. [26]. The event selection is made orthogonal to the 1-lepton analysis by requiring that events contain no leptons. Events containing electrons (muons) with p_T> 20(10) GeV and $|\eta| < 2.5(2.4)$ are rejected. Six or more jets with p_T> 80, 80, 35, 35, 35, 35 GeV and $|\eta| < 2.5$ are required, and two or more jets are required to be b-tagged. The minimum azimuthal separation between any of the three highest p_T jets and the direction of the missing transverse momentum is required to be greater than 0.2π. Top quarks are reconstructed in the same manner as was used for the hadronic top in the 1-lepton channel. Two tops are required, with the three-jet masses required to be between 80 and 270 GeV.

The main observables used to define the signal regions are:

- the missing transverse momentum, E_T^{miss};
- the transverse mass variable, $m_T^b = \sqrt{2 \times p_{T,b} \times E_T^{miss} \times (1 - \cos(\Delta\phi))}$ where $\Delta\phi$ is the angular separation of E_T^{miss} and the b-tagged jet closest in azimuth to the E_T^{miss}.

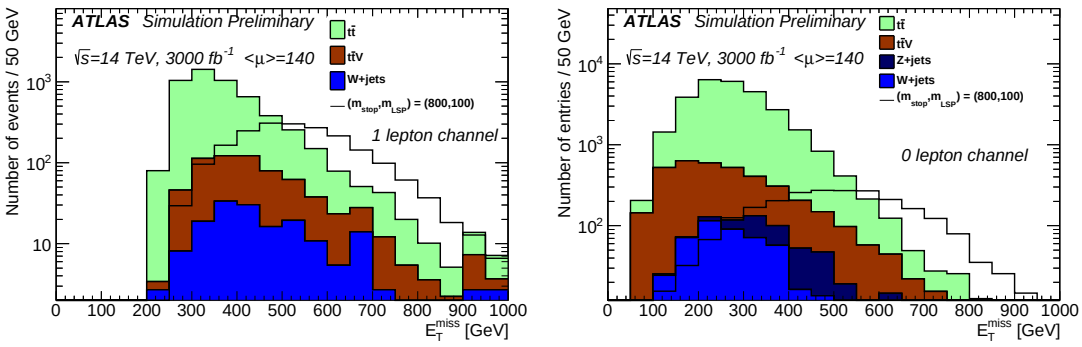

Figure 3: Left: the $E_{\mathrm{T}}^{\mathrm{miss}}$ distribution after all other requirements have been applied in the 1-lepton channel. Right: the $E_{\mathrm{T}}^{\mathrm{miss}}$ distribution after all other requirements have been applied in the 0-lepton analysis. The figures show the pair production of stops with a mass of 800 GeV decaying to a neutralino of 100 GeV as a signal.

The requirements on $E_{\mathrm{T}}^{\mathrm{miss}}$ and on m_{T}^{b} were examined across the plane of stop and LSP masses. Table 3 shows the minimum requirements on $E_{\mathrm{T}}^{\mathrm{miss}}$ and m_{T}^{b} as a function of the stop mass. Numbers of events for signal and background are shown in Table 4.

Figure 3 (right) shows the $E_{\mathrm{T}}^{\mathrm{miss}}$ distribution after all other requirements have been applied, for an assumed integrated luminosity of 3000 fb^{-1}. The most important background is from semileptonic $t\bar{t}$ events. Backgrounds from $t\bar{t}$+V (where $V = W, Z$) and from $Z(\rightarrow \nu\bar{\nu})$+jets processes are also significant. The $t\bar{t}$+V background is dominated by $t\bar{t}$+Z events.

	300 fb^{-1}		3000 fb^{-1}	
m_{stop} (GeV)	$E_{\mathrm{T}}^{\mathrm{miss}}$ (GeV)	m_{T}^{b} (GeV)	$E_{\mathrm{T}}^{\mathrm{miss}}$ (GeV)	m_{T}^{b} (GeV)
500	400	200	400	250
600	450	200	500	250
700	550	250	550	250
800	600	250	650	250
900	650	250	700	250
1000	650	300	800	400
1100	650	300	800	400
1200	650	300	900	450
1300	650	300	900	450
1400	650	300	900	450
1500	650	300	900	450

Table 3: Minimum requirements on $E_{\mathrm{T}}^{\mathrm{miss}}$ and m_{T}^{b} for the 0-lepton stop analysis as a function of the stop mass, for integrated luminosities of 300 and 3000 fb^{-1}.

2.4 Expected Sensitivity

Figure 4 shows the discovery and exclusion potential versus the $\tilde{t}$ and $\tilde{\chi}_1^0$ masses in the two studies together with the observed limits from the analyses of 8 TeV data [27, 28].

	(800,100)	(1100,100)
$t\bar{t}$	69±13	5.7±3.4
$t\bar{t}$+W	5±1	0.8±0.6
$t\bar{t}$+Z	38±5	3.9±1.5
W+jets	3±3	negligible
Z+jets	14±4	1.8±1.3
Total bkg	129±15	12.2±3.9
Signal	457±13	46.0±1.4

Table 4: Numbers of events for background and two representative signal points in the 0-lepton channel stop search for an integrated luminosity of 3000 fb^{-1}. The column headings indicate the masses of the stop and of the LSP, m($\tilde{t}$,$\tilde{\chi}_1^0$), in GeV. The selection criteria are optimized for the different stop masses. Estimates are based on MC only and uncertainties are statistical only.

In order for a signal point to be excluded at least five signal events are required to remain after the selection.

Figure 5 shows the discovery and exclusion potential for the combination of 1-lepton and 0-lepton analyses. The signal and background events of the two analyses were added for the combination. For LSP masses below approximately 200 GeV a stop discovery at 5σ would be possible with 3000 fb^{-1}for stop masses up to approximately 1.2 TeV, assuming a branching ratio of $\tilde{t} \rightarrow t + \tilde{\chi}_1^0$ of 100%. For a signal uncertainty of 20% (uncorrelated with the background uncertainty) the limits change by about 50 GeV. The discovery reach is extended by approximately 200 GeV by increasing the integrated luminosity from 300 fb^{-1}to 3000 fb^{-1}.

Several limitations of this study should be noted. The application of a tau veto [27, 28], not simulated in this study, will help to improve the signal-to-background ratio. For highly compressed scenarios, a more sophisticated analysis utilizing, for example, the information on the shape of the two-dimensional distribution of m_{T} versus $E_{\mathrm{T}}^{\mathrm{miss}}$ [27] is required. Other discriminating variables, such as those employed in Ref. [27], could further increase the sensitivity. For large stop masses, the sensitivity can be improved with better top reconstruction techniques for boosted top quarks.

3 Search for the associated production of $\tilde{\chi}_1^{\pm}$ and $\tilde{\chi}_2^0$

Based on naturalness arguments the $\tilde{\chi}_1^{\pm}$, $\tilde{\chi}_2^0$, and $\tilde{\chi}_1^0$ are also expected to have masses in the hundreds of GeV range [24, 25] and are potentially within reach of the LHC. The cross-section of $\tilde{\chi}_1^{\pm}$-$\tilde{\chi}_2^0$ associated production ranges from 1000 fb to 1 fb for masses between 200 GeV and 600 GeV and can dominate the SUSY production in scenarios with heavy squarks and gluinos. In this study both $\tilde{\chi}_1^{\pm}$ and $\tilde{\chi}_2^0$ are assumed to be wino-like while the $\tilde{\chi}_1^0$ is bino-like. The $\tilde{\chi}_1^{\pm}$ and $\tilde{\chi}_2^0$ masses are assumed to be equal. The $\tilde{\chi}_1^{\pm}$ is assumed to decay as $\tilde{\chi}_1^{\pm} \rightarrow W^{\pm(*)}\tilde{\chi}_1^0$ and the $\tilde{\chi}_2^0$ as $\tilde{\chi}_2^0 \rightarrow Z^{(*)}\tilde{\chi}_1^0$ with 100% branching ratio. The final state can contain three leptons and missing transverse momentum as shown in Figure 6.

3.1 Background Processes

The background for a signal with three leptons and large $E_{\mathrm{T}}^{\mathrm{miss}}$ is dominated by the irreducible processes $WZ^{(*)}$, tribosons and $t\bar{t} + Z/W$. The reducible process $t\bar{t}$ is also an important background, mimicking the signal when one of the b-quarks in the event decays semileptonically and is mis-identified as a prompt isolated lepton.

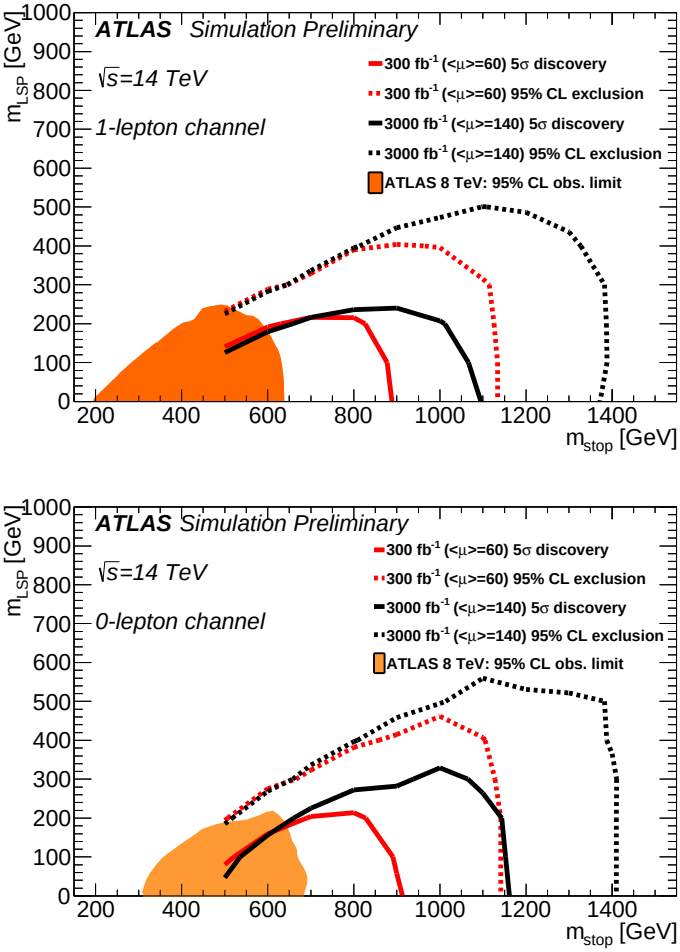

Figure 4: The 95% CL exclusion limits (dashed) and 5σ discovery reach (solid) for 300 fb^{-1} (red) and 3000 fb^{-1} (black) in the $\tilde{t}, \tilde{\chi}_1^0$ mass plane assuming $\tilde{t} \to t + \tilde{\chi}_1^0$ with a branching ratio of 100%. Upper: 1-lepton channel. Lower: 0-lepton channel. The observed limits from the analyses of 8 TeV data are also shown.

3.2 Event Pre-selection

Events are selected if they contain at least three candidate leptons[3] with p_{T} larger than 10 GeV and $|\eta| <$ 2.5 (2.4) for electrons (muons). Leptons are required to be isolated by imposing that the scalar sum of the transverse momenta of tracks within a cone of $\Delta R = 0.3$ around the lepton candidate, excluding the lepton candidate track itself, be less than 15% of the lepton p_{T}. All leptons are required to be separated from each other and from candidate jets. The latter requirement is imposed to suppress the background from semi-leptonic decays of heavy-flavor quarks. This source of background is further suppressed by vetoing events containing a b-jet candidate.

[3]In the following, leptons refer to electrons and muons including those from the τ-lepton decays but do not include hadronically-decaying τ-leptons

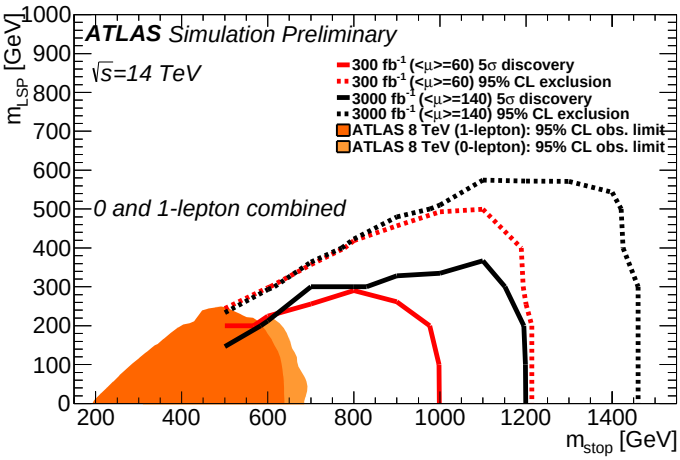

Figure 5: The 95% CL exclusion limits (dashed) and 5σ discovery reach (solid) for 300 fb^{-1} (red) and 3000 fb^{-1} (black) in the $\tilde{t}$, $\tilde{\chi}_1^0$ mass plane assuming $\tilde{t} \rightarrow t + \tilde{\chi}_1^0$ with a branching ratio of 100%. The results are shown for the combination of the 1-lepton and 0-lepton analyses. The observed limits from the analyses of 8 TeV data are also shown.

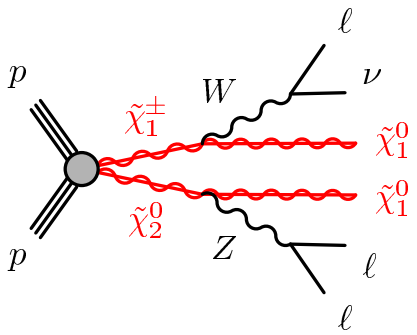

Figure 6: The Feynman diagram for the $\tilde{\chi}_2^0\tilde{\chi}_1^\pm$ simplified model studied in this note. The $\tilde{\chi}_1^\pm$ is assumed to decay as $\tilde{\chi}_1^\pm \rightarrow W^{\pm(*)}\tilde{\chi}_1^0$ and the $\tilde{\chi}_2^0$ as $\tilde{\chi}_2^0 \rightarrow Z^{(*)}\tilde{\chi}_1^0$ with 100% branching ratio.

3.3 Signal Region Selection

Two signal regions are defined for each luminosity scenario considered, "SR1-3000" and "SR2-3000" for the 3000 fb^{-1} scenario and "SR1-300" and "SR2-300" for the 300 fb^{-1} scenario. The regions are Z-enriched regions to target the $\tilde{\chi}_2^0$ decays via on-shell Z bosons and have ranked selections on the p_{T} of the three leptons of 100, 80 and 50 GeV from leading to second leading to third leading respectively. Events are required to include at least one Z boson candidate, defined as a Same-Flavour Opposite-Sign (SFOS) lepton pair with mass $|m_{\mathrm{SFOS}} - m_Z| < 10$ GeV. The m_{T} is constructed from the lepton not included in the SFOS pair with invariant mass closes to the Z boson mass. Each signal region has tight m_{T} and $E_{\mathrm{T}}^{\mathrm{miss}}$ requirements to increase sensitivity in scenarios with large mass splitting between the chargino (or $\tilde{\chi}_2^0$) and the lightest neutralino. The $E_{\mathrm{T}}^{\mathrm{miss}}$ and m_{T} distributions after the above selections and after requiring $E_{\mathrm{T}}^{\mathrm{miss}} > 50$ GeV, are shown in Figure 7 for the 3000 fb^{-1} scenario. The signal regions for the 300 fb^{-1} and 3000 fb^{-1} scenarios have been optimised seperately and are described in Table 5.

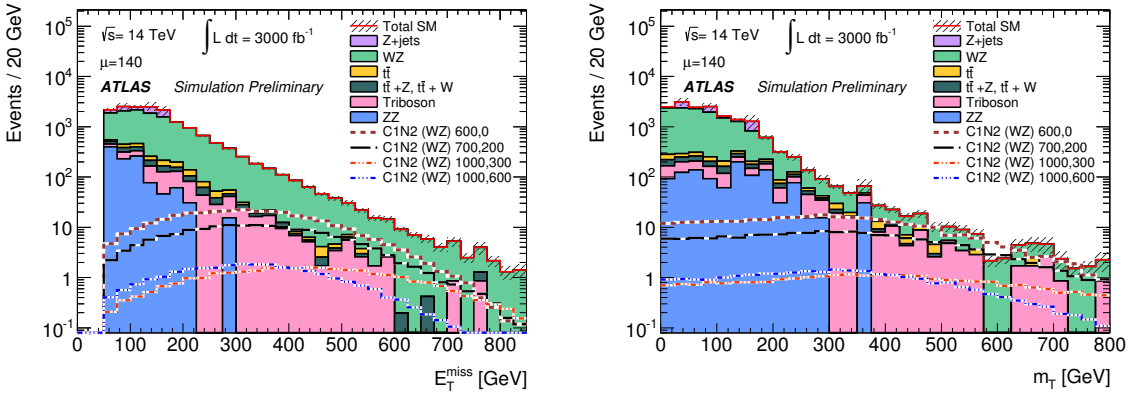

(a) $E_{\mathrm{T}}^{\mathrm{miss}}$ at 3000 fb^{-1}

(b) m_{T} at 3000 fb^{-1}

Figure 7: The (a) $E_{\mathrm{T}}^{\mathrm{miss}}$ and (b) m_{T} distribution in three-lepton events with a SFOS lepton pair, a Z boson candidate, a b-jet veto, $E_{\mathrm{T}}^{\mathrm{miss}} > 50$ GeV, lepton $p_T(1,2,3) > 100, 80, 50$ GeV in the 3000 fb^{-1} scenario. The figure shows signal model lines for $\tilde{\chi}_1^{\pm}\tilde{\chi}_2^0$ production with different mass assumptions for the $\tilde{\chi}_1^{\pm}$,$\tilde{\chi}_2^0$ and $\tilde{\chi}_1^0$.

Selection	SR1-300	SR2-300	SR1-3000	SR2-3000
m_{SFOS}[GeV]	81.2-101.2	81.2-101.2	81.2-101.2	81.2-101.2
# b-tagged jets	0	0	0	0
lepton p_T (1,2,3)[GeV]	$> 100, 80, 50$	$> 100, 80, 50$	$> 100, 80, 50$	$> 100, 80, 50$
m_{T} [GeV]	> 100	> 200	> 200	> 200
$E_{\mathrm{T}}^{\mathrm{miss}}$[GeV]	> 300	> 300	> 300	> 600

Table 5: Selection requirements for the 300 fb^{-1} and 3000 fb^{-1} signal regions. For each luminosity scenario, the signal regions are made disjoint in order that they can be combined. The mass of the SFOS lepton pair closest to the Z boson mass is denoted by m_{SFOS}.

3.4 Expected Sensitivity

The number of events for the SM background and two SUSY scenarios can be seen in Table 6 for 300 fb^{-1} and Table 7 for 3000 fb^{-1}.

The significances from the two signal regions are combined in quadrature for each of the two luminosities considered. The 95% exclusion contours that would be expected in the absence of a gaugino signal can be seen in Figure 8. For 300 fb^{-1}, the exclusion contour reaches 750 GeV in $\tilde{\chi}_1^{\pm}$,$\tilde{\chi}_2^0$ mass. For the high luminosity scenario with 3000 fb^{-1}, the contour extends as far as 1.1 TeV in $\tilde{\chi}_1^{\pm}$,$\tilde{\chi}_2^0$ mass.

4 Additional sensitivity estimates based upon projections of the results from 8 TeV SUSY searches to the high luminosity LHC

In order to study the high luminosity reach of the ATLAS experiment for some other example SUSY scenarios not covered with a complete 14 TeV analysis a simple projection strategy is used. The background and SUSY signal expectations in the signal regions measured at 8 TeV are scaled to 300 (3000) fb^{-1} at 14 TeV by reweighting the background predictions with the ratio of cross sections times integrated

Table 6: Numbers of events for SM and SUSY processes at different stages of the 3ℓ event selection for $\sqrt{s}$ = 14TeV and $\int Ldt = 300\,\text{fb}^{-1}$. Estimates are based on MC only and uncertainties are statistical only.

	SR1-300	SR2-300
WZ	11.1±0.3	3.9±0.2
tribosons	4.5±0.6	2.8±0.5
$t\bar{t}$+V	3.4±1.7	1.1±1.0
$t\bar{t}$	0.2±0.1	0.1±0.1
Σ SM	19.3±1.9	8.0±1.1
m($\tilde{\chi}_1^\pm$,$\tilde{\chi}_1^0$)=(300,100) GeV	9.0±0.5	3.5±0.3
m($\tilde{\chi}_1^\pm$,$\tilde{\chi}_1^0$)=(700,0) GeV	10.2±0.1	9.2±0.1

Table 7: Numbers of events for SM and SUSY processes at different stages of the 3ℓ event selection for $\sqrt{s}$ = 14TeV and $\int Ldt = 3000\,\text{fb}^{-1}$. Estimates are based on MC only and uncertainties are statistical only.

	SR1-3000	SR2-3000
WZ	49.6±2.3	3.7±0.6
tribosons	33.4±5.3	0.9±0.9
$t\bar{t}$+V	1.4±0.7	< 0.5
$t\bar{t}$	1.6±1.1	< 0.9
Σ SM	86.0±5.9	4.6±1.1
m($\tilde{\chi}_1^\pm$,$\tilde{\chi}_1^0$)=(500,0) GeV	195.5±2.9	7.1±0.5
m($\tilde{\chi}_1^\pm$,$\tilde{\chi}_1^0$)=(1000,0) GeV	20.2±0.2	6.9±0.1

luminosity.

Several assumptions are made in the simplification. The effect of the increasing number of pile up events at high luminosity LHC is neglected. This effect yields an overestimation of the reach in the SUSY mass compared to a complete analysis. To reoptimize for a 14 TeV analysis at 300 (3000) fb^{-1} the main selection cut of the analysis is tightened compared to the 8 TeV analysis. The shapes of the background and signal distributions can change due to different centre-of-mass energies which would result in different selection efficiencies. Therefore a PDF dependent reweighting from $\sqrt{s}$ = 8 TeV to $\sqrt{s}$ = 14 TeV is applied on the dominant backgrounds.

The pair production of charginos and the production of sbottom squarks are investigated. Results for the 8 TeV search for the $\tilde{\chi}_1^\pm\tilde{\chi}_1^\mp$ pair production decaying into $W^+\tilde{\chi}_1^0 W^-\tilde{\chi}_1^0$ for the $e\mu$ channel are described in Ref. [30]. The final state consists of two leptons, missing transverse momentum and no hadronic activity. This study assumes that the efficiency and acceptance of the background and signal selection do not change at the HL-LHC compared to the 8 TeV analysis. Estimates of the exclusion and discovery reach comparing 300 and 3000 fb^{-1} yield an increase of the discovery reach in chargino mass from 250 to 400 GeV for chargino pair production.

The pair production of sbottoms which decay with 100% branching ratio to $b\tilde{\chi}_1^0$ is also investigated. The 8 TeV, 20.7 fb^{-1} analysis results in Ref. [31] are extrapolated to 14 TeV scenarios with integrated luminosities of 300 fb^{-1} and 3000 fb^{-1}. PDF reweighting is used to reweight the dominant background contributions. This projection for the pair production of sbottom quarks yields improvements of the

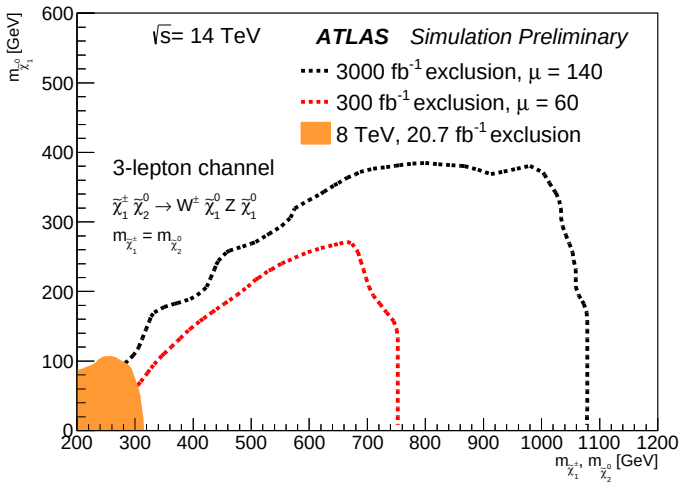

Figure 8: The 95 % CL exclusion limits for 300 fb^{-1} (dashed) and 3000 fb^{-1} (solid line) in the $\tilde{\chi}_1^{\pm}\tilde{\chi}_2^0$ mass plane via a WZ signal. The shaded area corresponds to the 8 TeV limits from the ATLAS three-lepton analysis [29].

discovery reach from ~1050 to ~1250 GeV comparing 300 and 3000 fb^{-1}.

5 Conclusions

The sensitivity to heavy SUSY particles will be increased significantly when the centre-of-mass-energy of the LHC reaches a value close to the design of $\sqrt{s} = 14$ TeV. Feasibility studies on two benchmark SUSY scenarios, stop pair production and chargino neutralino production, are carried out with 14 TeV MC samples and by applying detector response corrections to generator level particles. An increase of integrated luminosity from 300 fb^{-1} to 3000 fb^{-1} extends the sensitivity potential for stop quarks decaying in top and $\tilde{\chi}_1^0$ by about 200 GeV, and by about 300 GeV for $\tilde{\chi}_1^{\pm}\tilde{\chi}_2^0$ production assuming $\tilde{\chi}_1^{\pm}$ ($\tilde{\chi}_2^0$) decaying via W(Z) and $\tilde{\chi}_1^0$. In addition projections from existing 8 TeV analyses are pursued for pair production of sbottoms and pair production of charginos, showing improvements of the discovery reach by 200 GeV and 150 GeV for the two cases respectively. Future improvements in the understanding of experimental and theoretical systematic uncertainties on the SM background would provide additional potential for sensitivity gains at high luminosity on SUSY scenarios reported here and beyond.

References

[1] H. Miyazawa, Prog. Theor. Phys. **36** (1966) 1266.
P. Ramond, Phys. Rev. **D 3** (1971) 2415.
Y. Golfand, E. Likhtman, JETP Lett. **13** (1971) 323.
A. Neveu, J. H. Schwarz, Nucl. Phys. **B 31** (1971) 86.
A. Neveu, J. H. Schwarz, Phys. Rev. **D 4** (1971) 1109.
J. L. Gervais, B. Sakita, Nucl. Phys. **B 34** (1971) 632.
D. Volkov, V. Akulov, Phys. Lett. **B 46** (1973) 109.
J. Wess, B. Zumino, Phys. Lett. **B 49** (1974) 52.
J. Wess, B. Zumino, Nucl. Phys. **B 70** (1974) 39.

[2] ATLAS Collaboration, Phys.Lett. **B716** (2012) 1–29, arXiv:1207.7214.

[3] CMS Collaboration, Phys. Lett. B (2012) 30, arXiv:1207.7235.

[4] ATLAS Collaboration, JINST **3** (2008) S08003.

[5] ATLAS Collaboration, ATLAS-CONF-2013-024.
ATLAS Collaboration, ATLAS-CONF-2013-037.
ATLAS Collaboration, ATLAS-CONF-2013-093.
ATLAS Collaboration, ATLAS-CONF-2013-089.
ATLAS Collaboration, ATLAS-CONF-2013-069.
ATLAS Collaboration, ATLAS-CONF-2013-068.
ATLAS Collaboration, ATLAS-CONF-2013-065.
ATLAS Collaboration, ATLAS-CONF-2013-062.
ATLAS Collaboration, ATLAS-CONF-2013-061.
ATLAS Collaboration, ATLAS-CONF-2013-058.
ATLAS Collaboration, ATLAS-CONF-2013-057.
ATLAS Collaboration, ATLAS-CONF-2013-047.
ATLAS Collaboration, ATLAS-CONF-2013-048.
ATLAS Collaboration, ATLAS-CONF-2013-035.
ATLAS Collaboration, ATLAS-CONF-2013-036.
ATLAS Collaboration, ATLAS-CONF-2013-025.
ATLAS Collaboration, ATLAS-CONF-2013-026.
ATLAS Collaboration, ATLAS-CONF-2013-028.
ATLAS Collaboration, ATLAS-CONF-2013-007.
ATLAS Collaboration, arXiv:1308.2631.
ATLAS Collaboration, arXiv:1308.1841.

[6] ATLAS Collaboration, ATLAS-CONF-2013-047 (2013).

[7] ATLAS Collaboration, Phys.Rev.Lett. **109** (2012) 211803, arXiv:1208.2590 [hep-ex].

[8] ATLAS Collaboration, Phys.Lett. **B718** (2013) 841–859, arXiv:1208.3144 [hep-ex].

[9] ATLAS Collaboration, Phys.Lett. **B718** (2013) 879–901, arXiv:1208.2884 [hep-ex].

[10] ATLAS Collaboration, ATL-PHYS-PUB-2013-002.

[11] ATLAS Collaboration, ATL-PHYS-PUB-2013-009.

[12] T. Gleisberg *et al.*, JHEP **0902** (2009) 007, arXiv:0811.4622.

[13] M. Mangano *et al.*, JHEP **07** (2003) 001, arXiv:hep-ph/0206293.

[14] J. Alwall *et al.*, JHEP **06** (2011) 128. 1106.0522.

[15] M. Aliev *et al.*, Comput. Phys. Commun. **182** (2011) 1034, arXiv:1007.1327.

[16] K. Melnikov, F. Petriello, Phys. Rev. **D 74** (2006) 114017, arXiv:hep-ph/0609070.

[17] C. Anastasiou *et al.*, Phys. Rev. **D 69** (2004) 094008.

[18] J. Pumplin *et al.*, JHEP **0207** (012) 2002, arXiv:0802.0007.

[19] H. Lai *et al.*, Phys. Rev. **D 82** (2010) 074024, arXiv:1007.2241.

[20] M. Bahr et al., Eur. Phys. J. **C58** (2008) 639–707, arXiv:0803.0883 [hep-ph].

[21] T. Plehn, http://www.thphys.uni-heidelberg.de/˜ plehn/index.php?show=prospino.

[22] W. Beenakker *et al.*, JHEP. **1008** (2010) 098, arXiv:hep-ph/1006.4771.

[23] J. T. Linnemann, arXiv:physics:0312059.

[24] R. Barbieri and G. F. Giudice, Nucl.Phys. **B306** (1988) 63.

[25] B. de Carlos and J. A. Casas, Phys. Lett. **B309** (1993) 320–328, arXiv:hep-ph/9303291.

[26] ATLAS Collaboration, Phys.Rev.Lett. **109** (2012) 211802, arXiv:1208.1447 [hep-ex].

[27] ATLAS Collaboration, ATLAS-CONF-2013-037.

[28] ATLAS Collaboration, ATLAS-CONF-2013-024.

[29] ATLAS Collaboration, ATLAS-CONF-2013-035.

[30] ATLAS Collaboration, ATLAS-CONF-2013-049.

[31] ATLAS Collaboration, arXiv:1308.2631.